

Converting PT -Symmetric Topological Classes by Floquet Engineering

Ming-Jian Gao^{1,2} and Jun-Hong An^{1,2,*}

¹*School of Physical Science and Technology & Lanzhou Center for Theoretical Physics, Lanzhou University, Lanzhou 730000, China*

²*Key Laboratory of Quantum Theory and Applications of MoE & Key Laboratory of Theoretical Physics of Gansu Province, Lanzhou University, Lanzhou 730000, China*

Going beyond the conventional classification rule of Altland-Zirnbauer symmetry classes, PT symmetric topological phases are classified by $(PT)^2 = 1$ or -1 . The interconversion between the two PT -symmetric topological classes is generally difficult due to the constraint of $(PT)^2$. Here, we propose a scheme to control and interconvert the PT -symmetric topological classes by Floquet engineering. We find that it is the breakdown of the \mathbb{Z}_2 gauge, induced by the π phase difference between different hopping rates, by the periodic driving that leads to such an interconversion. Relaxing the system from the constraint of $(PT)^2$, rich exotic topological phases, e.g., the coexisting PT -symmetric first-order real Chern insulator and second-order topological insulators not only in different quasienergy gaps, but also in one single gap, are generated. In contrast to conventional Floquet topological phases, our result provides a way to realize exotic topological phases without changing symmetries. It enriches the family of topological phases and gives an insightful guidance for the development of multifunctional quantum devices.

Introduction.—As an indispensable and significant field in modern physics, topological phases which go beyond Landau symmetry-breaking theory not only enrich the paradigm of condensed matter physics, but also provide new directions for the development of quantum technology [1–6]. Including topological insulator [1, 2, 7–12], superconductor [2, 3, 13–15], and semimetal [5, 6, 16–19], topological phases are signified by the formation of symmetry-protected boundary states and can be characterized by topological invariants of the bulk energy bands. This, as one of the most significant features of topological phases, is called bulk-boundary correspondence. Symmetries play a dominant role in the classification of topological phases. Through three intrinsic time-reversal, chiral, and particle-hole symmetries, we can classify topological phases into the tenfold Altland-Zirnbauer symmetry classes [4, 20]. This has become the cornerstone for the development of topological phases.

It was recently found that the three intrinsic symmetries are insufficient to classify all topological phases. Crystal symmetry also plays a crucial role in many topological systems [21–27]. In particular, the topological phases with the combined space-time inversion (PT) symmetry do not obey the Altland-Zirnbauer classification rule [28–36]. The space inversion symmetry in the presence of the \mathbb{Z}_2 gauge field induced by the hopping amplitudes with phases 0 and π should be projectively represented, which alters the algebraic structure of the symmetries and thus generates rich exotic topological phases [37]. The PT -symmetric topological phases can be roughly divided into two categories with $(PT)^2 = \pm 1$ [38]. The systems with $(PT)^2 = -1$ host the Möbius topological insulator, in which the boundary spectra are twisted in momentum space [37, 39, 40], and the axion insulator, which exhibits a quantized magnetoelectric response [41, 42]. Possessing real Bloch wave functions,

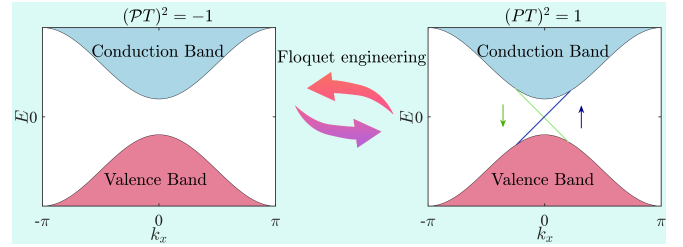


FIG. 1. Converting PT -symmetric topological classes by Floquet engineering. Two-dimensional PT -symmetric systems with $(PT)^2 = -1$ does not have the gapless edge states. The one with $(PT)^2 = 1$ allows the gapless edge states.

the PT -symmetric systems with $(PT)^2 = 1$ host the real Chern insulator [43], which is characterized by a \mathbb{Z}_2 topological invariant of the Stiefel-Whitney class [34, 44, 45], and the Euler topological phases, which have multi-gap topologies with band nodes carrying non-Abelian charges [46–50]. These advances indicate that the spatial inversion symmetry opens a door to the discovery of exotic topological phases. However, limited by the value of $(PT)^2$, the interconversion among these PT -symmetric topological phases is difficult. In practical application in designing multiplexing devices, it is generally desirable to exploit the respective advantages of the different classes of topological phases. A natural question is how to realize the interconversion between different PT -symmetric topological classes on demand. On the other hand, Floquet engineering has become a useful tool to create topological phases due to its distinguished role in changing symmetries of the systems [51–70]. Can Floquet engineering interconvert the topological classes, while still preserving the PT symmetry?

Addressing these problems, we here propose a scheme to convert the PT -symmetric topological class from

$(PT)^2 = -1$ to 1 by Floquet engineering. Our analysis reveals that it is the breakdown of the \mathbb{Z}_2 gauge that makes such a conversion realizable. Setting free from the constraint of $(PT)^2$, exotic PT -symmetric two-dimensional topological phases with coexisting first- and second-order topological insulators are realized not only in different quasienergy gaps but also in one single gap. They are completely absent in static PT -symmetric systems. Going beyond the conventional Floquet topological phases, our result lays a foundation to realize exotic topological phases without changing symmetries. The coexisting topological phases also have the potential to facilitate the design of multifunctional quantum devices.

Floquet PT -symmetric topological phases.—The Altland-Zirnbauer symmetry classes governed by three intrinsic symmetries do not exhaust the topological phases [38, 39, 43, 71, 72]. It was found that some topological phases are determined not only by the intrinsic symmetries but also the spatial symmetry. The topological phases with the combined symmetries of time reversal T and spatial inversion P are classified by whether $(PT)^2 = 1$ or -1 and the difference between the system dimension and the codimension of defect [4, 38]. Generally, $(PT)^2 = 1$ in spinless systems and -1 in spin-1/2 systems [38, 71]. On the other hand, if the hopping rates between different sublattices have a π phase difference, then an additional \mathbb{Z}_2 gauge is exerted in the system. It makes the PT operation be projectively represented [71]. According to the \mathbb{Z}_2 gauge theory, actual inversion operation becomes $\mathcal{P} = G\mathcal{P}$, where G is a gauge transformation satisfying

$$[G, T] = 0, \quad \{G, P\} = 0, \quad G^2 = 1. \quad (1)$$

Thus, the \mathbb{Z}_2 gauge facilitates the realization of topological phases with $(PT)^2 = -1$ in spinless systems and topological phases with $(PT)^2 = 1$ in spin-1/2 systems.

We propose a Floquet engineering scheme to interconvert the PT -symmetric topological phases in the presence of \mathbb{Z}_2 gauge between $(PT)^2 = 1$ and -1 . A minimal requirement is that the periodic driving must not break the PT symmetry. We use a two-step periodic driving protocol as

$$\mathcal{H}(\mathbf{k}, t) = \begin{cases} \mathcal{H}_1(\mathbf{k}), & t \in [n\mathcal{T}, n\mathcal{T} + \mathcal{T}_1) \\ \mathcal{H}_2(\mathbf{k}), & t \in [n\mathcal{T} + \mathcal{T}_1, (n+1)\mathcal{T}) \end{cases}, \quad (2)$$

where $n \in \mathbb{Z}$ and $\mathcal{T} = \mathcal{T}_1 + \mathcal{T}_2$ is the driving period. The time-periodic $\mathcal{H}(\mathbf{k}, t)$ does not have a well-defined energy spectrum. According to Floquet theorem, the one-period evolution operator $U_{\mathcal{T}} = e^{-i\mathcal{H}_2(\mathbf{k})\mathcal{T}_2}e^{-i\mathcal{H}_1(\mathbf{k})\mathcal{T}_1}$ defines an effective Hamiltonian $\mathcal{H}_{\text{eff}}(\mathbf{k}) = \frac{i}{\mathcal{T}} \ln U_{\mathcal{T}}$, whose eigenvalues are called quasienergies. The topological features of our periodic system are defined in the quasienergy spectrum. However, $\mathcal{H}_{\text{eff}}(\mathbf{k})$ does not inherit the time-reversal and chiral symmetries under the operations T and S of the static system due to

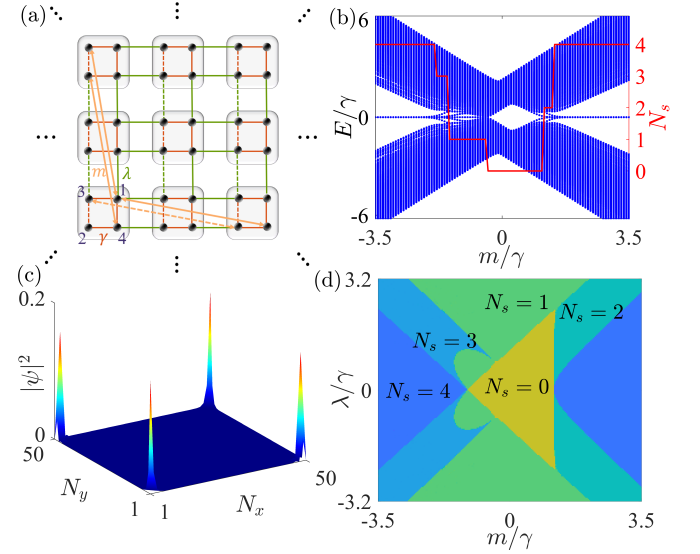


FIG. 2. (a) Scheme of our system. γ and λ are the intracell and nearest-neighbor intercell hopping rates, and m is the long-range one. The dashed lines denote the hopping rates with a π -phase difference from their solid counterparts. (b) Energy spectrum and chiral number N_s as a function of m , with $\lambda = 0.64\gamma$. (c) Distribution of the zero-mode state. (d) Phase diagram described by N_s .

$[\mathcal{H}_1(\mathbf{k}), \mathcal{H}_2(\mathbf{k})] \neq 0$. Defining two unitary transformations $F_l(\mathbf{k}) = e^{i(-1)^l \mathcal{H}_l(\mathbf{k})\mathcal{T}_l/2}$ ($l = 1, 2$), we find $\mathcal{T}_l U_{\mathcal{T}}(\mathbf{k})\mathcal{T}_l^{-1} = U_{\mathcal{T}}^\dagger(-\mathbf{k})$ and $\mathcal{S}_l U_{\mathcal{T}}(\mathbf{k})\mathcal{S}_l^{-1} = U_{\mathcal{T}}^{-1}(\mathbf{k})$, where $\mathcal{T}_l = F_l^{-1}(-\mathbf{k})T F_l(\mathbf{k})$ and $\mathcal{S}_l = F_l^{-1}(\mathbf{k})S F_l(\mathbf{k})$. It means that $\mathcal{H}_{\text{eff}}(\mathbf{k})$ possesses the time-reversal symmetry $\mathcal{T}_l \mathcal{H}_{\text{eff}}(\mathbf{k})\mathcal{T}_l^{-1} = \mathcal{H}_{\text{eff}}^\dagger(-\mathbf{k})$ and the chiral symmetry $\mathcal{S}_l \mathcal{H}_{\text{eff}}(\mathbf{k})\mathcal{S}_l^{-1} = -\mathcal{H}_{\text{eff}}(\mathbf{k})$ under the redefined time-reversal and chiral operations \mathcal{T}_l and \mathcal{S}_l . The above results indicate that the intrinsic symmetries of the static system are fully inherited by our periodically driven system. Thus, it is natural to expect that the periodic driving could not generate exotic topological phases according to the conventional rule of the Altland-Zirnbauer symmetry classification [4].

It is surprising to find that the \mathbb{Z}_2 gauge would be broken by the periodic driving that satisfies $[G, \mathcal{T}_l] \neq 0$. It causes the PT symmetry class in our periodic system to go back to the original case, i.e., $(PT)^2 = 1$ in spinless system and $(PT)^2 = -1$ in spin-1/2 system. Therefore, we realize an inter-conversion of the PT -symmetric topological phases between $(PT)^2 = \pm 1$ via manipulating the gauge by Floquet engineering. In contrast to the widely used scheme to induce topological phase transitions between different Altland-Zirnbauer symmetry classes by changing the intrinsic symmetries [59, 73–75], our scheme opens another avenue to explore exotic topological phases by changing the PT symmetry class via the \mathbb{Z}_2 gauge induced by the π phase difference between different hopping rates. From an application perspective, it lays a

foundation for designing quantum devices based on such conveniently controllable phases.

Extended Benalcazar-Bernevig-Hughes model.—We propose a two-dimensional spinless fermion square lattice system to realize the inter-conversion of the PT -symmetric topological classes. It is Benalcazar-Bernevig-Hughes model with long-range hoppings, see Fig. 2(a). Its momentum-space Hamiltonian reads $H = \sum_{\mathbf{k}} C_{\mathbf{k}}^\dagger \mathcal{H}(\mathbf{k}) C_{\mathbf{k}}$ with $C_{\mathbf{k}}^\dagger = (C_{\mathbf{k},1}^\dagger \ C_{\mathbf{k},2}^\dagger \ C_{\mathbf{k},3}^\dagger \ C_{\mathbf{k},4}^\dagger)$ and [76]

$$\mathcal{H}(\mathbf{k}) = \mathbf{d}(\mathbf{k}) \cdot \boldsymbol{\Gamma}, \quad (3)$$

where $d_1(\mathbf{k}) = -(\lambda \sin k_y + m \sin 2k_x)$, $d_2(\mathbf{k}) = -(\gamma + \lambda \cos k_y + m \cos 2k_x)$, $d_3(\mathbf{k}) = -(\lambda \sin k_x + m \sin 2k_y)$, $d_4(\mathbf{k}) = 0$, and $d_5(\mathbf{k}) = \gamma + \lambda \cos k_x + m \cos 2k_y$. γ is the intracell hopping rate, λ is the intercell hopping rate, m is the long-range hopping rate, $\Gamma_i = \tau_y \sigma_i$ ($i = 1, 2, 3$), $\Gamma_4 = \tau_z \sigma_0$, and $\Gamma_5 = \tau_x \sigma_0$, with τ_i and σ_i being Pauli matrices, τ_0 and σ_0 being identity matrices. The system possesses the intrinsic particle-hole $\mathcal{C} = \tau_z \sigma_0 K$, time-reversal $T = K$, with K being the complex conjugation, and chiral $S = \tau_z \sigma_0$ symmetries. According to the Altland-Zirnbauer classification rule, the system belongs to the BDI class and is topologically trivial in first order [4]. The external inversion operation of the system is $P = \tau_0 \sigma_x$, which cannot make the system invariant. Because of the presence of the π phase difference between different hopping rates, the system has an additional \mathbb{Z}_2 gauge and the gauge transformation $G = \tau_0 \sigma_z$ satisfies Eq. (1). Therefore, the operation under which the PT symmetry is respected is $\mathcal{PT} = GPT = i\tau_0 \sigma_y K$, which obeys $(\mathcal{PT})^2 = -1$. According to the classification rule of the PT -symmetric topological phases, the system only hosts the second-order topological phases [38, 71]. The chiral symmetry makes the real-space Hamiltonian H of this system unitarily equivalent to $H' = \begin{pmatrix} 0 & D \\ D^\dagger & 0 \end{pmatrix}$. Thus, the lattice in the real space is split into two sublattices labeled by A and B . Its second-order topological phase is described by the chiral number [76]

$$N_s = \frac{1}{2\pi i} \text{Tr} \log(\mathcal{Q}_A \mathcal{Q}_B^\dagger), \quad (4)$$

where $\mathcal{Q}_p = \mathcal{U}_p^\dagger Q_p \mathcal{U}_p$ and $Q_p = \sum_{\mathbf{R}, \beta \in p} c_{\mathbf{R}, \beta}^\dagger |0\rangle \exp(-i \frac{2\pi x y}{L_x L_y}) \langle 0| c_{\mathbf{R}, \beta}$ are the sublattice quadrupole moment operators, with $p = A, B$ and $c_{\mathbf{R}, \beta}^\dagger$ being the creation operator of the fermion in the p sublattice of the unit cell $\mathbf{R} = (x, y)$. The unitary transformation $\mathcal{U}_p = (\psi_1^p, \psi_2^p, \dots, \psi_M^p)$, with $DD^\dagger \psi_n^A = \epsilon_n^2 \psi_n^A$, $D^\dagger D \psi_n^B = \epsilon_n^2 \psi_n^B$, and $M = 2L_x L_y$, is performed to project Q_p in the space spanned by $\{\psi_n^p\}$. The energy spectrum under the open-boundary condition in Fig. 2(b) reveals that $4|N_s|$ degenerate gapped zero-mode states are formed. The widely tunable N_s with the change of m originates from the long-range hoppings of our model. The probability distribution of these zero-mode states in Fig. 2(c)

confirms their second-order nature. The phase diagram in Fig. 2(d) gives a global picture of the topological phases. Our result verifies that the system only hosts the second-order topological phases. It agrees with the classification rule of the PT -symmetric topological phase with $(\mathcal{PT})^2 = -1$.

To generate rich PT -symmetric topological phases, we intend to convert the symmetry class into the one with $(\mathcal{PT})^2 = 1$. We apply a periodic driving on the hopping rate m as

$$m(t) = \begin{cases} m_1, & t \in [n\mathcal{T}, n\mathcal{T} + \mathcal{T}_1) \\ m_2, & t \in [n\mathcal{T} + \mathcal{T}_1, (n+1)\mathcal{T}) \end{cases} \quad (5)$$

$\mathcal{H}_{\text{eff}}(\mathbf{k})$ has the time-reversal and chiral symmetries under the redefined operations \mathcal{T}_l and \mathcal{S}_l . It is straightforward to prove $[G, \mathcal{T}_l] \neq 0$. Thus, the \mathbb{Z}_2 gauge is broken and $\mathcal{P} = GP$ cannot describe the inversion operation for the periodic system anymore. The space-time inversion symmetry of the periodically driven system goes back to the one of the original case $(P\mathcal{T}_l)^2 = 1$, which results in $P = I$, with I being the momentum inversion operation [38, 71]. Therefore, we realize the conversion of the PT -symmetric topological phases from $(\mathcal{PT})^2 = -1$ to 1 via breaking the gauge by periodic driving. This is impossible in static systems. It is noted that the conventional Altland-Zirnbauer topological classification of the system does not change because the three intrinsic symmetries are fully inherited in our periodic system. This endows our work with a substantial difference from the traditional Floquet topological states, where periodic driving induces exotic topological phases mainly by changing the intrinsic symmetries of the systems [23, 51, 63–66, 70, 77].

According to the classification rule of the PT -symmetric topological phases [38], our periodic system with $(P\mathcal{T}_l)^2 = 1$ supports the first-order real Chern insulators and the second-order topological insulators. Furthermore, the topological phases of the periodic system occur not only at the quasienergy zero but also at $|\pi/\mathcal{T}|$. Thus, setting the PT -symmetric topological phases free from the constraint of $(P\mathcal{T}_l)^2 = -1$, extremely rich topological phases emerge in our periodic system. Now, we develop a complete characterization of them. First, making two unitary transformations $F_l(\mathbf{k})$ on $\mathcal{U}_{\mathcal{T}}(\mathbf{k})$, we can define two Hamiltonians $\mathbb{H}_{\text{eff}, l}(\mathbf{k}) = i\mathcal{T}^{-1} \ln[F_l(\mathbf{k}) \mathcal{U}_{\mathcal{T}}(\mathbf{k}) F_l^\dagger(\mathbf{k})]$, which have the same quasienergy spectrum as $\mathcal{H}_{\text{eff}}(\mathbf{k})$. In the similar manner as Eq. (4) in the static system, we define two chiral numbers $N_{s, l}$ in $\mathbb{H}_{\text{eff}, l}(\mathbf{k})$. The second-order topological phases of the periodic system in the zero and $|\pi/\mathcal{T}|$ modes are described by $N_\alpha = (N_{s, 1} + e^{i\alpha} N_{s, 2})/2$, with $\alpha = 0$ and π [54]. Second, the first-order topological phases of this PT -symmetric system are characterized by real Chern number [43, 78]

$$\mathcal{V}_R = \frac{-i}{4\pi} \int_{\text{BZ}} d^2 \mathbf{k} \text{Tr}[\tau_y \sigma_0 (\nabla_{\mathbf{k}} \times \mathcal{A})_z] \mod 2, \quad (6)$$

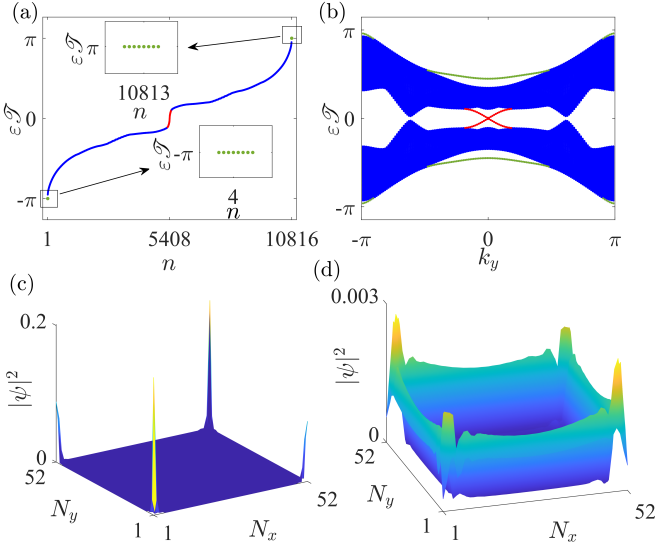


FIG. 3. Quasienergies under the open boundary conditions of (a) the x and y directions and (b) only the x direction. The red line in (a) and (b) represent the gapless boundary states. The green point in (a) and line in (b) represent the gapped corner states. Distributions of (c) the gapped $|\pi/\mathcal{T}|$ -mode state and (d) the gapless zero-mode state. We use $\lambda = 0.64\gamma$, $m_1 = -0.36\gamma$, $m_2 = 3.6\gamma$, $\mathcal{T}_1 = 1.2\gamma^{-1}$ and $\mathcal{T}_2 = 0.6\gamma^{-1}$.

where $\mathcal{A}_{mn} = \langle m, \mathbf{k} | \nabla_{\mathbf{k}} | n, \mathbf{k} \rangle$ and $|m/n, \mathbf{k}\rangle$ are the real eigenstates of $\mathcal{H}_{\text{eff}}(\mathbf{k})$ under the reality requirement $PT|m/n, \mathbf{k}\rangle = |m/n, \mathbf{k}\rangle$.

Figure 3(a) shows the quasienergies of the periodic system in the open boundary condition. We can clearly find that sixteen gapped corner states appear in the $|\pi/\mathcal{T}|$ modes and a pair of gapless boundary states appear in the zero mode. The quasienergies in Fig. 3(b) under the x -direction open boundary condition prove that the first-order gapless boundary states occur in the zero mode and the second-order gapped corner states occur in the $|\pi/\mathcal{T}|$ mode. This is further confirmed by the probability distribution of the π/\mathcal{T} - and zero-gap states in Fig. 3(c) and 3(d). Calculating the chiral numbers and the real Chern number, we obtain $N_0 = 0$, $N_\pi = 4$, and $\mathcal{V}_R = 1$. They quantify the $4|N_\pi|$ second-order corner states in the $|\pi/\mathcal{T}|$ mode and \mathcal{V}_R pair of first-order boundary state in the zero mode. Therefore, we realize the coexistence of the first-order real Chern insulator in the zero mode and the second-order topological insulator in the $|\pi/\mathcal{T}|$ mode in a PT symmetric system via converting its symmetry class from $(PT)^2 = -1$ to 1 by the periodic driving.

Next, the periodic driving also makes the first- and second-order topological phases coexist even in a same quasienergy gap. Figure 4(a) shows the quasienergies under the open boundary condition of the x and y directions. It can be seen that, in addition to the gapped $|\pi/\mathcal{T}|$ mode, the corner states are also present in the quasienergy band of the gapless boundary states of zero mode. This is confirmed by the quasienergies under the

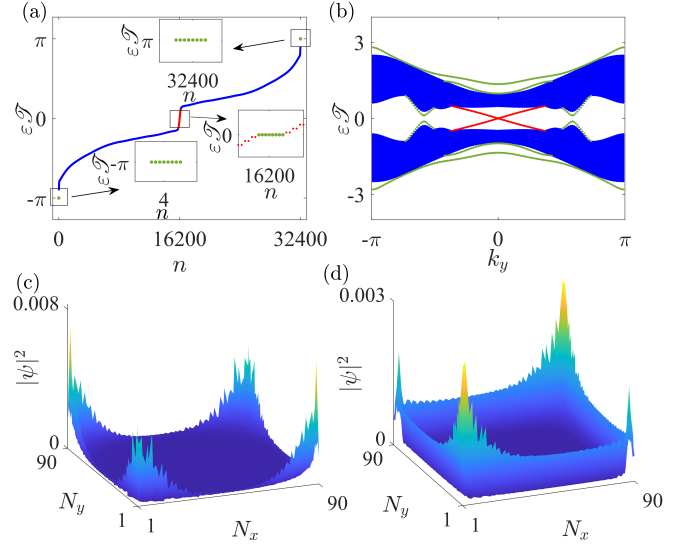


FIG. 4. (a) Quasienergies under the open boundary conditions of (a) the x and y directions and (b) only the x direction. The red line in (a) and (b) represent the gapless boundary states. The green point in (a) and line in (b) represent the gapped corner states. Distribution of (c) the zero-mode corner state and (d) boundary state. We use $\lambda = 0.64\gamma$, $m_1 = -0.1\gamma$, $m_2 = 3.6\gamma$, $\mathcal{T}_1 = 1.2\gamma^{-1}$ and $\mathcal{T}_2 = 0.6\gamma^{-1}$.

x -direction open boundary condition in Fig. 4(b). The probability distribution of the state with quasienergy zero in Fig. 4(c) shows the feature of the second-order corner mode. The one of the state with quasienergy nearest to zero in Fig. 4(d) shows clearly the feature of the first-order boundary mode. They verify the coexistence of the boundary and corner states at the zero gap. When we compute the topological invariants, we obtain $N_0 = -2$, $N_\pi = 4$, and $\mathcal{V}_R = 1$. They indicate that eight second-order corner states and a pair of first-order gapless boundary states coexist in the zero gap and sixteen second-order corner states exist in the $|\pi/\mathcal{T}|$ gap. Thus, we achieve the coexistence of the first- and second-order topological insulators in a same gap by Floquet engineering. Such an exotic PT symmetric topological phase cannot be realized in static PT -symmetric systems.

Discussion and conclusion.—It is noted that although only the step-like driving protocol is considered, our scheme is generalizable to other driving protocols. The PT -symmetric topological phases have been realized in photonic, acoustic, and electronic systems [39, 72, 79–82]. Floquet engineering has become a versatile tool for generating novel topological phases in various platforms [70, 83–92]. These progresses give a strong support to the experimental realization of our scheme.

In summary, we have proposed a scheme to convert the PT -symmetric topological phases from $(PT)^2 = -1$ to 1 by Floquet engineering. Breaking through the constraint of $(PT)^2 = -1$, we have discovered diverse exotic PT -symmetric phases with coexisting first- and

second-order topological insulators not only in different quasienergy gaps but also in one single quasienergy gap. They are completely absent in the corresponding static system. Our study reveals that it is the breakdown of the \mathbb{Z}_2 gauge by the periodic driving that causes the inter-conversion between different symmetry classes. Without changing any symmetry, our scheme has a substantial difference from the conventional Floquet engineering, which pursues exotic topological phases by breaking the intrinsic symmetries. Enriching the family of PT -symmetric topological phases, our result opens an avenue to controllably explore novel topological phases and to design quantum devices by simultaneously utilizing the respective advantages of different orders of topological phases.

Acknowledgments.—The work is supported by the National Natural Science Foundation of China (Grants No. 124B2090, No. 12275109, and No. 12247101), the Innovation Program for Quantum Science and Technology of China (Grant No. 2023ZD0300904), the Fundamental Research Funds for the Central Universities (Grant No. lzujbky-2024-jdzz06), and the Natural Science Foundation of Gansu Province (No. 22JR5RA389).

* anjhong@lzu.edu.cn

- [1] M. Z. Hasan and C. L. Kane, Colloquium: Topological insulators, *Rev. Mod. Phys.* **82**, 3045 (2010).
- [2] X.-L. Qi and S.-C. Zhang, Topological insulators and superconductors, *Rev. Mod. Phys.* **83**, 1057 (2011).
- [3] S. R. Elliott and M. Franz, Colloquium: Majorana fermions in nuclear, particle, and solid-state physics, *Rev. Mod. Phys.* **87**, 137 (2015).
- [4] C.-K. Chiu, J. C. Y. Teo, A. P. Schnyder, and S. Ryu, Classification of topological quantum matter with symmetries, *Rev. Mod. Phys.* **88**, 035005 (2016).
- [5] N. P. Armitage, E. J. Mele, and A. Vishwanath, Weyl and Dirac semimetals in three-dimensional solids, *Rev. Mod. Phys.* **90**, 015001 (2018).
- [6] B. Q. Lv, T. Qian, and H. Ding, Experimental perspective on three-dimensional topological semimetals, *Rev. Mod. Phys.* **93**, 025002 (2021).
- [7] A. Tiwari, M.-H. Li, B. A. Bernevig, T. Neupert, and S. A. Parameswaran, Unhinging the surfaces of higher-order topological insulators and superconductors, *Phys. Rev. Lett.* **124**, 046801 (2020).
- [8] R.-X. Zhang, F. Wu, and S. Das Sarma, Möbius insulator and higher-order topology in $\text{MnBi}_{2n}\text{Te}_{3n+1}$, *Phys. Rev. Lett.* **124**, 136407 (2020).
- [9] R. Chen, C.-Z. Chen, J.-H. Gao, B. Zhou, and D.-H. Xu, Higher-order topological insulators in quasicrystals, *Phys. Rev. Lett.* **124**, 036803 (2020).
- [10] Q. Wei, X. Zhang, W. Deng, J. Lu, X. Huang, M. Yan, G. Chen, Z. Liu, and S. Jia, 3D hinge transport in acoustic higher-order topological insulators, *Phys. Rev. Lett.* **127**, 255501 (2021).
- [11] J. Du, T. Li, X. Fan, Q. Zhang, and C. Qiu, Acoustic realization of surface-obstructed topological insulators, *Phys. Rev. Lett.* **128**, 224301 (2022).
- [12] W. Jia, X.-C. Zhou, L. Zhang, L. Zhang, and X.-J. Liu, Unified characterization for higher-order topological phase transitions, *Phys. Rev. Res.* **5**, L022032 (2023).
- [13] X. Zhu, Second-order topological superconductors with Mixed Pairing, *Phys. Rev. Lett.* **122**, 236401 (2019).
- [14] Y. Volpez, D. Loss, and J. Klinovaja, Second-order topological superconductivity in π -junction Rashba layers, *Phys. Rev. Lett.* **122**, 126402 (2019).
- [15] F. Schindler, B. Bradlyn, M. H. Fischer, and T. Neupert, Pairing obstructions in topological superconductors, *Phys. Rev. Lett.* **124**, 247001 (2020).
- [16] H.-X. Wang, Z.-K. Lin, B. Jiang, G.-Y. Guo, and J.-H. Jiang, Higher-order Weyl semimetals, *Phys. Rev. Lett.* **125**, 146401 (2020).
- [17] S. A. A. Ghorashi, T. Li, and T. L. Hughes, Higher-order Weyl semimetals, *Phys. Rev. Lett.* **125**, 266804 (2020).
- [18] T. Liu, J. J. He, Z. Yang, and F. Nori, Higher-order Weyl-exceptional-ring semimetals, *Phys. Rev. Lett.* **127**, 196801 (2021).
- [19] Z. Pu, H. He, L. Luo, Q. Ma, L. Ye, M. Ke, and Z. Liu, Acoustic higher-order Weyl semimetal with bound hinge states in the continuum, *Phys. Rev. Lett.* **130**, 116103 (2023).
- [20] A. Bansil, H. Lin, and T. Das, Colloquium: Topological band theory, *Rev. Mod. Phys.* **88**, 021004 (2016).
- [21] W. A. Benalcazar, B. A. Bernevig, and T. L. Hughes, Quantized electric multipole insulators, *Science* **357**, 61 (2017).
- [22] Y. Tanaka, T. Zhang, M. Uwaha, and S. Murakami, Anomalous crystal shapes of topological crystalline insulators, *Phys. Rev. Lett.* **129**, 046802 (2022).
- [23] X.-L. Du, R. Chen, R. Wang, and D.-H. Xu, Weyl nodes with higher-order topology in an optically driven nodal-line semimetal, *Phys. Rev. B* **105**, L081102 (2022).
- [24] Q. Wei, X. Zhang, W. Deng, J. Lu, X. Huang, M. Yan, G. Chen, Z. Liu, and S. Jia, Higher-order topological semimetal in acoustic crystals, *Nature Materials* **20**, 812 (2021).
- [25] C. Chen, X.-T. Zeng, Z. Chen, Y. X. Zhao, X.-L. Sheng, and S. A. Yang, Second-order real nodal-line semimetal in three-dimensional graphdiyne, *Phys. Rev. Lett.* **128**, 026405 (2022).
- [26] H. Kondo and Y. Akagi, Dirac surface states in magnonic analogs of topological crystalline insulators, *Phys. Rev. Lett.* **127**, 177201 (2021).
- [27] J. Kruthoff, J. de Boer, J. van Wezel, C. L. Kane, and R.-J. Slager, Topological classification of crystalline insulators through band structure combinatorics, *Phys. Rev. X* **7**, 041069 (2017).
- [28] J. Ahn, S. Park, and B.-J. Yang, Failure of Nielsen-Ninomiya theorem and fragile topology in two-dimensional systems with space-time inversion symmetry: Application to twisted bilayer graphene at magic angle, *Phys. Rev. X* **9**, 021013 (2019).
- [29] X.-L. Sheng, C. Chen, H. Liu, Z. Chen, Z.-M. Yu, Y. X. Zhao, and S. A. Yang, Two-dimensional second-order topological insulator in graphdiyne, *Phys. Rev. Lett.* **123**, 256402 (2019).
- [30] T. Ozawa, H. M. Price, A. Amo, N. Goldman, M. Hafezi, L. Lu, M. C. Rechtsman, D. Schuster, J. Simon, O. Zilberberg, and I. Carusotto, Topological photonics, *Rev. Mod. Phys.* **91**, 015006 (2019).
- [31] Z. Yang, F. Gao, X. Shi, X. Lin, Z. Gao, Y. Chong, and B. Zhang, Topological acoustics, *Phys. Rev. Lett.* **114**,

- 114301 (2015).
- [32] J.-T. Wang, J.-X. Liu, H.-T. Ding, and P. He, Proposal for implementing Stiefel-Whitney insulators in an optical raman lattice, *Phys. Rev. A* **109**, 053314 (2024).
 - [33] M. Takeichi, R. Furuta, and S. Murakami, Morse theory study on the evolution of nodal lines in PT-symmetric nodal-line semimetals, *Phys. Rev. B* **107**, 085139 (2023).
 - [34] Z. Song, T. Zhang, and C. Fang, Diagnosis for nonmagnetic topological semimetals in the absence of spin-orbital coupling, *Phys. Rev. X* **8**, 031069 (2018).
 - [35] Q. Wu, A. A. Soluyanov, and T. Bzdušek, Non-Abelian band topology in noninteracting metals, *Science* **365**, 1273 (2019).
 - [36] Q. Guo, T. Jiang, R.-Y. Zhang, L. Zhang, Z.-Q. Zhang, B. Yang, S. Zhang, and C. T. Chan, Experimental observation of non-Abelian topological charges and edge states, *Nature* **594**, 195 (2021).
 - [37] Y. X. Zhao, Y.-X. Huang, and S. A. Yang, \mathbb{Z}_2 -projective translational symmetry protected topological phases, *Phys. Rev. B* **102**, 161117 (2020).
 - [38] Y. X. Zhao, A. P. Schnyder, and Z. D. Wang, Unified theory of PT and CP invariant topological metals and nodal superconductors, *Phys. Rev. Lett.* **116**, 156402 (2016).
 - [39] T. Li, J. Du, Q. Zhang, Y. Li, X. Fan, F. Zhang, and C. Qiu, Acoustic Möbius insulators from projective symmetry, *Phys. Rev. Lett.* **128**, 116803 (2022).
 - [40] H. Xue, Z. Wang, Y.-X. Huang, Z. Cheng, L. Yu, Y. X. Foo, Y. X. Zhao, S. A. Yang, and B. Zhang, Projectively enriched symmetry and topology in acoustic crystals, *Phys. Rev. Lett.* **128**, 116802 (2022).
 - [41] P. Tang, Q. Zhou, G. Xu, and S.-C. Zhang, Dirac fermions in an antiferromagnetic semimetal, *Nature Physics* **12**, 1100 (2016).
 - [42] J.-X. Qiu, C. Tzschaschel, J. Ahn, A. Gao, H. Li, X.-Y. Zhang, B. Ghosh, C. Hu, Y.-X. Wang, Y.-F. Liu, D. Bérubé, T. Dinh, Z. Gong, S.-W. Lien, S.-C. Ho, B. Singh, K. Watanabe, T. Taniguchi, D. C. Bell, H.-Z. Lu, A. Bansil, H. Lin, T.-R. Chang, B. B. Zhou, Q. Ma, A. Vishwanath, N. Ni, and S.-Y. Xu, Axion optical induction of antiferromagnetic order, *Nature Materials* **22**, 583 (2023).
 - [43] K. Wang, J.-X. Dai, L. B. Shao, S. A. Yang, and Y. X. Zhao, Boundary criticality of PT -invariant topology and second-order nodal-line semimetals, *Phys. Rev. Lett.* **125**, 126403 (2020).
 - [44] J. Ahn, D. Kim, Y. Kim, and B.-J. Yang, Band topology and linking structure of nodal line semimetals with \mathbb{Z}_2 monopole charges, *Phys. Rev. Lett.* **121**, 106403 (2018).
 - [45] S. J. Yue, Q. Liu, S. A. Yang, and Y. X. Zhao, Stability and noncentered PT symmetry of real topological phases, *Phys. Rev. B* **109**, 195116 (2024).
 - [46] Q. Wu, A. A. Soluyanov, and T. Bzdušek, Non-Abelian band topology in noninteracting metals, *Science* **365**, 1273–1277 (2019).
 - [47] F. N. Ünal, A. Bouhon, and R.-J. Slager, Topological euler class as a dynamical observable in optical lattices, *Phys. Rev. Lett.* **125**, 053601 (2020).
 - [48] Q. Guo, T. Jiang, R.-Y. Zhang, L. Zhang, Z.-Q. Zhang, B. Yang, S. Zhang, and C. T. Chan, Experimental observation of non-Abelian topological charges and edge states, *Nature* **594**, 195–200 (2021).
 - [49] B. Jiang, A. Bouhon, Z.-K. Lin, X. Zhou, B. Hou, F. Li, R.-J. Slager, and J.-H. Jiang, Experimental observation of non-abelian topological acoustic semimetals and their phase transitions, *Nature Physics* **17**, 1239 (2021).
 - [50] B. Peng, A. Bouhon, B. Monserrat, and R.-J. Slager, Phonons as a platform for non-Abelian braiding and its manifestation in layered silicates, *Nature Communications* **13**, 423 (2022).
 - [51] Q.-J. Tong, J.-H. An, J. Gong, H.-G. Luo, and C. H. Oh, Generating many Majorana modes via periodic driving: A superconductor model, *Phys. Rev. B* **87**, 201109(R) (2013).
 - [52] H. Liu, T.-S. Xiong, W. Zhang, and J.-H. An, Floquet engineering of exotic topological phases in systems of cold atoms, *Phys. Rev. A* **100**, 023622 (2019).
 - [53] H. Wu and J.-H. An, Floquet topological phases of non-Hermitian systems, *Phys. Rev. B* **102**, 041119(R) (2020).
 - [54] H. Wu, B.-Q. Wang, and J.-H. An, Floquet second-order topological insulators in non-Hermitian systems, *Phys. Rev. B* **103**, L041115 (2021).
 - [55] L. Li, C. H. Lee, and J. Gong, Realistic Floquet semimetal with exotic topological linkages between arbitrarily many nodal loops, *Phys. Rev. Lett.* **121**, 036401 (2018).
 - [56] Y. Peng and G. Refael, Floquet second-order topological insulators from nonsymmorphic space-time symmetries, *Phys. Rev. Lett.* **123**, 016806 (2019).
 - [57] H. Hu, B. Huang, E. Zhao, and W. V. Liu, Dynamical singularities of Floquet higher-order topological insulators, *Phys. Rev. Lett.* **124**, 057001 (2020).
 - [58] B. Huang and W. V. Liu, Floquet higher-order topological insulators with anomalous dynamical polarization, *Phys. Rev. Lett.* **124**, 216601 (2020).
 - [59] T. Nag, V. Juričić, and B. Roy, Hierarchy of higher-order Floquet topological phases in three dimensions, *Phys. Rev. B* **103**, 115308 (2021).
 - [60] B.-Q. Wang, H. Wu, and J.-H. An, Engineering exotic second-order topological semimetals by periodic driving, *Phys. Rev. B* **104**, 205117 (2021).
 - [61] M. Jangjan and M. V. Hosseini, Floquet engineering of topological metal states and hybridization of edge states with bulk states in dimerized two-leg ladders, *Scientific Reports* **10**, 14256 (2020).
 - [62] Y. Peng, Floquet higher-order topological insulators and superconductors with space-time symmetries, *Phys. Rev. Res.* **2**, 013124 (2020).
 - [63] H. Dehghani, M. Hafezi, and P. Ghaemi, Light-induced topological superconductivity via Floquet interaction engineering, *Phys. Rev. Res.* **3**, 023039 (2021).
 - [64] D. Yates, Y. Lemonik, and A. Mitra, Central charge of periodically driven critical Kitaev chains, *Phys. Rev. Lett.* **121**, 076802 (2018).
 - [65] Z. Yan and Z. Wang, Tunable Weyl points in periodically driven nodal line semimetals, *Phys. Rev. Lett.* **117**, 087402 (2016).
 - [66] A. K. Ghosh, T. Nag, and A. Saha, Floquet generation of a second-order topological superconductor, *Phys. Rev. B* **103**, 045424 (2021).
 - [67] M.-J. Gao, Y.-P. Ma, and J.-H. An, Majorana modes and their Floquet engineering in a trapped-ion system, *Phys. Rev. B* **109**, 184518 (2024).
 - [68] P. He and Z.-H. Huang, Floquet engineering and simulating exceptional rings with a quantum spin system, *Phys. Rev. A* **102**, 062201 (2020).
 - [69] A. K. Ghosh, T. Nag, and A. Saha, Floquet second order topological superconductor based on unconventional

- pairing, *Phys. Rev. B* **103**, 085413 (2021).
- [70] J. W. McIver, B. Schulte, F.-U. Stein, T. Matsuyama, G. Jotzu, G. Meier, and A. Cavalleri, Light-induced anomalous Hall effect in graphene, *Nat. Phys.* **16**, 38 (2020).
 - [71] Y. X. Zhao, C. Chen, X.-L. Sheng, and S. A. Yang, Switching spinless and spinful topological phases with projective PT symmetry, *Phys. Rev. Lett.* **126**, 196402 (2021).
 - [72] Y. Meng, S. Lin, B.-j. Shi, B. Wei, L. Yang, B. Yan, Z. Zhu, X. Xi, Y. Wang, Y. Ge, S.-q. Yuan, J. Chen, G.-G. Liu, H.-x. Sun, H. Chen, Y. Yang, and Z. Gao, Spinful topological phases in acoustic crystals with projective \mathcal{PT} symmetry, *Phys. Rev. Lett.* **130**, 026101 (2023).
 - [73] T.-S. Xiong, J. Gong, and J.-H. An, Towards large-Chern-number topological phases by periodic quenching, *Phys. Rev. B* **93**, 184306 (2016).
 - [74] M. S. Rudner, N. H. Lindner, E. Berg, and M. Levin, Anomalous edge states and the bulk-edge correspondence for periodically driven two-dimensional systems, *Phys. Rev. X* **3**, 031005 (2013).
 - [75] A. Eckardt, Colloquium: Atomic quantum gases in periodically driven optical lattices, *Rev. Mod. Phys.* **89**, 011004 (2017).
 - [76] W. A. Benalcazar and A. Cerjan, Chiral-symmetric higher-order topological phases of matter, *Phys. Rev. Lett.* **128**, 127601 (2022).
 - [77] F. Qin, C. H. Lee, and R. Chen, Light-induced phase crossovers in a quantum spin Hall system, *Phys. Rev. B* **106**, 235405 (2022).
 - [78] Y. X. Zhao and Y. Lu, PT -symmetric real Dirac fermions and semimetals, *Phys. Rev. Lett.* **118**, 056401 (2017).
 - [79] X. Xiang, Y.-G. Peng, F. Gao, X. Wu, P. Wu, Z. Chen, X. Ni, and X.-F. Zhu, Demonstration of acoustic higher-order topological stiefel-whitney semimetal, *Phys. Rev. Lett.* **132**, 197202 (2024).
 - [80] Y. Han, C. Cui, X.-P. Li, T.-T. Zhang, Z. Zhang, Z.-M. Yu, and Y. Yao, Cornertronics in two-dimensional second-order topological insulators, *Phys. Rev. Lett.* **133**, 176602 (2024).
 - [81] H. Xue, Z. Y. Chen, Z. Cheng, J. X. Dai, Y. Long, Y. X. Zhao, and B. Zhang, Stiefel-whitney topological charges in a three-dimensional acoustic nodal-line crystal, *Nature Communications* **14**, 4563 (2023).
 - [82] Y. Pan, C. Cui, Q. Chen, F. Chen, L. Zhang, Y. Ren, N. Han, W. Li, X. Li, Z.-M. Yu, H. Chen, and Y. Yang, Real higher-order weyl photonic crystal, *Nature Communications* **14**, 6636 (2023).
 - [83] F. Mahmood, C.-K. Chan, Z. Alpichshev, D. Gardner, Y. Lee, P. A. Lee, and N. Gedik, Selective scattering between Floquet-Bloch and Volkov states in a topological insulator, *Nat. Phys.* **12**, 306 (2016).
 - [84] K. Wintersperger, C. Braun, F. N. Ünal, A. Eckardt, M. D. Liberto, N. Goldman, I. Bloch, and M. Aidelsburger, Realization of an anomalous Floquet topological system with ultracold atoms, *Nat. Phys.* **16**, 1058 (2020).
 - [85] P. Roushan, C. Neill, A. Megrant, Y. Chen, R. Babush, R. Barends, B. Campbell, Z. Chen, B. Chiaro, A. Dunsworth, A. Fowler, E. Jeffrey, J. Kelly, E. Lucero, J. Mutus, P. J. J. O'Huallachain, M. Neeley, C. Quintana, D. Sank, A. Vainsencher, J. Wenner, T. White, E. Kapit, H. Neven, and J. Martinis, Chiral ground-state currents of interacting photons in a synthetic magnetic field, *Nat. Phys.* **13**, 146 (2017).
 - [86] M. C. Rechtsman, J. M. Zeuner, Y. Plotnik, Y. Lumer, D. Podolsky, F. Dreisow, S. Nolte, M. Segev, and A. Szameit, Photonic Floquet topological insulators, *Nature* **496**, 196 (2013).
 - [87] S. Mukherjee, A. Spracklen, M. Valiente, E. Andersson, P. Öhberg, N. Goldman, and R. R. Thomson, Experimental observation of anomalous topological edge modes in a slowly driven photonic lattice, *Nat. Commun.* **8**, 13918 (2017).
 - [88] L. J. Maczewsky, J. M. Zeuner, S. Nolte, and A. Szameit, Observation of photonic anomalous Floquet topological insulators, *Nat. Commun.* **8**, 13756 (2017).
 - [89] Q. Cheng, Y. Pan, H. Wang, C. Zhang, D. Yu, A. Gover, H. Zhang, T. Li, L. Zhou, and S. Zhu, Observation of anomalous π modes in photonic Floquet engineering, *Phys. Rev. Lett.* **122**, 173901 (2019).
 - [90] F. Meinert, M. J. Mark, K. Lauber, A. J. Daley, and H.-C. Nägerl, Floquet engineering of correlated tunneling in the Bose-Hubbard model with ultracold atoms, *Phys. Rev. Lett.* **116**, 205301 (2016).
 - [91] Z. Cheng, R. W. Bomantara, H. Xue, W. Zhu, J. Gong, and B. Zhang, Observation of $\pi/2$ modes in an acoustic Floquet system, *Phys. Rev. Lett.* **129**, 254301 (2022).
 - [92] Z. Lin, W. Song, L.-W. Wang, H. Xin, J. Sun, S. Wu, C. Huang, S. Zhu, J.-H. Jiang, and T. Li, Observation of topological transition in Floquet non-Hermitian skin effects in silicon photonics, *Phys. Rev. Lett.* **133**, 073803 (2024).